Large-scale brain networks account for sustained and transient activity during target detection

Dante Mantini[a,b,*], **Maurizio Corbetta**[a,b,c,d], **Mauro Gianni Perrucci**[a,b], **Gian Luca Romani**[a,b], and **Cosimo Del Gratta**[a,b]

[a]Institute for Advanced Biomedical Technologies, "G. D'Annunzio University" Foundation, "G. D'Annunzio" University, 66013 Chieti, Italy

[b]Department of Clinical Sciences and Bio-imaging, "G. D'Annunzio" University, Chieti, Italy

[c]Department of Neurology, Washington University, St. Louis, Missouri, USA

[d]Department of Radiology, Washington University, St. Louis, Missouri, USA

Abstract

Target detection paradigms have been widely applied in the study of human cognitive functions, particularly those associated with arousal, attention, stimulus processing and memory. In EEG recordings, the detection of task-relevant stimuli elicits the P300 component, a transient response with latency around 300 ms. The P300 response has been shown to be affected by the amount of mental effort and learning, as well as habituation. Furthermore, trial-by-trial variability of the P300 component has been associated with inter-stimulus interval, target-to-target interval or target probability; however, understanding the mechanisms underlying this variability is still an open question. In order to investigate whether it could be related to the distinct cortical networks in which coherent intrinsic activity is organized, and to understand the contribution of those networks to target detection processes, we carried out a simultaneous EEG–fMRI study, collecting data from 13 healthy subjects during a visual oddball task. We identified five large-scale networks, that largely overlap with the dorsal attention, the ventral attention, the core, the visual and the sensory-motor networks. Since the P300 component has been consistently associated with target detection, we concentrated on the first two brain networks, the time-course of which showed a modulation with the P300 response as detected in simultaneous EEG recordings. A trial-by-trial EEG–fMRI correlation approach revealed that they are involved in target detection with different functional roles: the ventral attention network, dedicated to revealing salient stimuli, was transiently activated by the occurrence of targets; the dorsal attention network, usually engaged during voluntary orienting, reflected sustained activity, possibly related to search for targets.

Keywords

Electroencephalography (EEG); Functional magnetic resonance imaging (fMRI); Multimodal imaging; P300; Oddball paradigm; Target detection

---

[*]Corresponding author. Fax: +39 0871 3556 930. d.mantini@unich.it (D. Mantini).

Introduction

Target detection studies have been widely applied in the study of cognitive functions, since they have been shown to reflect arousal, attention, stimulus processing and memory operations (Polich and Herbst, 2000). They are performed by means of acoustic, visual or somatosensory oddball tasks, in which the subject responds to target stimuli that occur infrequently and irregularly within a series of standard stimuli. The detection of these task-relevant stimuli is associated in the EEG recordings with the P300 component, a transient activity with latency between 250 and 550 ms (Picton, 1992). The amplitude of the P300 component has been shown to be generally affected, in healthy subjects, by the amount of mental effort and learning, as well as habituation (Lew and Polich, 1993; Polich and Kok, 1995). In addition, although the underlying mechanisms for the abnormal P300 component are unknown, this evoked response has proved to be an important tool in neuropsychiatric research for the investigation of many disorders that influence the central nervous system (CNS) function, including schizophrenia (Blackwood, 2000), Alzheimer's disease (Muscoso et al., 2006), and Parkinson's disease (Katsarou et al., 2004).

In order to define which cerebral structures are involved in the P300 generation, several methodologies have been employed, among which intracranial recordings (Halgren et al., 1998), EEG/MEG (Basile et al., 1997; Tarkka and Stokic, 1998) and fMRI (Clark et al., 2000; Kiehl et al., 2005). It has been suggested that the large number of activated areas, mainly found in frontal, temporal and parietal cortices, might belong to different functional systems that are simultaneously active during target detection (Bledowski et al., 2004a; Horn et al., 2003). In the perspective of gaining further information about the dynamics of these systems, the fusion of EEG and fMRI has been recently suggested, because it might in principle allow to combine the high spatial and temporal resolution of fMRI and EEG respectively (Mulert et al., 2004; Calhoun et al., 2006; Eichele et al., 2008).

The most common approach for the EEG–fMRI integration is based on the use of spatial constraints, where information from the location of fMRI activation is used for event-related potential (ERP) source reconstruction (Bledowski et al., 2004b; Mulert et al., 2004). An interesting method for direct ERP/fMRI fusion has been recently proposed by Calhoun et al. (2006). However, methods based on ERP analysis do not use the valuable information that can be provided by concurrent EEG and fMRI data (Debener et al., 2006; Eichele et al., 2005, 2008; Benar et al., 2007; Strobel et al., 2008). In fact, only simultaneous recordings protocols capture the temporal dynamics in both modalities, and therefore provide a unique means for the study of EEG–fMRI coupling. From this standpoint, simultaneous EEG–fMRI can be considered a promising technique for the analysis of single-trial responses to rare and frequent events during the oddball task (Benar et al., 2007).

Recent fMRI studies on cerebral connectivity have shown that it is possible to identify multiple highly specific functional networks, which largely account for intrinsic activity (De Luca et al., 2006; Damoiseaux et al., 2006; Mantini et al., 2007b) and are related to trial-by-trial variability in evoked responses (Fox et al., 2006). In target detection studies, activations within the ventral attention network, specialized for the detection of behaviorally relevant

stimuli, were consistently observed when comparing the brain responses to target and non-target events (Bledowski et al., 2004a; Calhoun et al., 2006). We further hypothesized that the dorsal attention network, recently found to be dedicated to adaptive task control in a resting state functional connectivity study (Dosenbach et al., 2007), might be engaged during search for targets, hence playing an important role in target detection performance. From this standpoint, the trial-by-trial variability of the P300 amplitude, documented in several EEG studies (Barry et al., 2000; Croft et al., 2003; Gonsalvez and Polich, 2002), might be considered an electrophysiological correlate of ongoing adaptive processes associated with target detection. In addition, other neuroimaging studies provided evidence for the existence of the core network, a functional system dedicated to stable task control and primarily including insula and anterior cingulate cortex (Dosenbach et al., 2006, 2007), which can be assumed to be engaged during target detection as well.

Despite the large number of studies on ongoing and task-related brain activity in different behavioral conditions, little is known on how intrinsic variability relates to and is comparable with event-related responses, both in EEG (Arieli et al., 1996; Makeig et al., 2002, 2004) and fMRI (Fair et al., 2007; Fox et al., 2006, 2007; Fox and Raichle, 2007). Nonetheless, recent oddball studies suggested that a better understanding of the cerebral processes underlying target detection could be achieved by means of the single-trial analysis of the P300 responses (Benar et al., 2007; Eichele et al., 2005, 2008). On the basis of the above findings, we propose that this variability could be related to the distinct cortical networks in which coherent intrinsic activity is organized, and particularly to the ventral and dorsal attention networks. In order to understand their different contribution to target detection, as well as their link to the P300 response fluctuations, we investigated the ongoing cerebral responses during a visual oddball paradigm by means of simultaneous EEG–fMRI.

Material and methods

Subjects and task design

Thirteen healthy subjects (all right-handed male, age 23.2±4.6 years) with no prior history of neurological injury were enrolled. Before undergoing the examination, they gave their written informed consent to the experimental procedures, which were approved by the local Institutional Ethics Committee. The study consisted of a visual oddball paradigm, with the presentation of 80% of frequent stimuli and 20% of rare stimuli respectively. The subjects were asked to count the rare events and to report their number at the end of the session. The stimuli consisted of yellow (frequent events) and blue (rare events) disks, appearing on a black background with 200 ms duration, and presented in random order every 2.5 s (Supplementary Fig. 1). The visual images were prepared using the Cogent 2000 toolbox (www.vislab.ucl.ac.uk), running in the MATLAB (The Mathworks Inc., Natick, MA, USA) programming environment. They were generated by a NEC projector (NEC Corporation, Tokyo, Japan) working at 60 Hz refreshment rate, projected outside the scanner onto a translucent screen placed at the end of the scanner bore, and visible to the subject via a mirror attached to the head coil. Since the time instant of the stimulus presentation could be delayed with respect to the trigger delivery (time range 50–100 ms), the exact stimulation

timing was monitored by means of a photoelectric cell placed onto the screen. The simultaneous EEG–fMRI recording lasted about 8 min.

EEG–fMRI acquisition

The EEG recordings were acquired with a 32-channel MR-compatible BrainAmp system (Brainproducts, Munich, Germany). All the electrodes, integrated into the BrainCap cap, were ring-type sintered nonmagnetic Ag/AgCl electrodes. Twenty-nine EEG electrodes were placed on the scalp according to the 10% system. The reference electrode was positioned in correspondence of the Fcz electrode, between electrodes Fz and Cz. The ground electrode was placed between electrodes Fpz and Fz. Three additional electrodes were dedicated to the acquisition of electrocardiogram (EKG) and electrooculogram (EOG). The impedance was maintained close to 5 kΩ by means of an electrode paste. The resolution and dynamic range of the EEG acquisition system were 100 nV and ± 3.2 mV, respectively. Data were collected with a sampling rate of 5 kHz; band-pass filtering from 0.016 to 250 Hz was applied.

Magnetic resonance imaging was performed using a 1.5 T Siemens Magnetom Vision Scanner with a standard quadrature head coil. Functional images were acquired by means of T2*-weighted echo planar imaging (EPI) free induction decay (FID) sequences with the following parameters: TE 60 ms, matrix size 64×64, FOV 256 mm, in-plane voxel size 4 mm×4 mm, flip angle 90°, slice thickness 7 mm and no gap. Each fMRI volume, acquired with a volume TR of 2500 ms and a scan time of 1620 ms, consisted of 16 bicommissural slices. After the functional study, a high resolution structural volume was acquired via a 3D MPRAGE sequence (sagittal slices, matrix 256×256, FOV 256 mm, slice thickness 1 mm, no gap, in-plane voxel size 1 mm×1 mm, flip angle 12°, TR=9.7 ms, TE=4 ms) in order to provide the anatomical reference for the functional scan.

Artifact attenuation in EEG data

The EEG recordings were re-referenced to the average of TP9 and TP10 channels, positioned close to the subject's mastoids (digitally linked mastoids reference). A modified version of the adaptive artifact subtraction (AAS) algorithm was used for off-line correction of imaging artifact (Allen et al., 2000; Gonçalves et al., 2007): after the detection of each fMRI slice onset from EEG data, slice artifact waveforms were segmented, averaged, and iteratively subtracted from the EEG signals (Gonçalves et al., 2007). Subsequently, the EEG data were downsampled to 1 kHz and filtered between 0.5 and 40 Hz by means of a Chebychev II-type filter with 40 dB attenuation and zerophase distortion. Simulated signals for ballistocardiographic (BCG), slice MRI and volume MRI artifacts were generated, using information from acquired data. An average BCG waveform was constructed by differentiating the EKG signal, detecting QRS peak timing, and averaging with respect to QRS peaks. The BCG template was then obtained by replicating the same averaged waveform across heart beats, shifted by a fixed delay of 150 ms in order to take into account the typical difference in timing between EKG and BCG signals. Volume MRI and slice MRI artifact templates were created by means of signal peaks, positioned in correspondence of volume and slice onset times, respectively (Fig. 1). Independent component analysis (ICA) was used for the for the decomposition of the EEG data into a set of independent spatio-temporal patterns (independent components, ICs) (Hyvärinen and Oja, 2000), and the

subsequent removal of BCG, imaging and ocular artifacts (Fig. 1). The FastICA algorithm (Hyvärinen et al., 1999) was run on the 29 EEG signals for the decomposition into 29 ICs (Makeig et al., 1997), which were then automatically classified into brain signals and artifacts, on the basis of the correlation coefficient r_t with the set of EEG artifact templates, including EKG and EOG recordings, simulated BCG, volume MRI and slice MRI artifacts. A specific IC was considered artifactual in case of $r_t > 0.2$ for at least an EEG artifact template. With this procedure, from 8 to 14 artifactual ICs were typically detected, and subtracted from the EEG recordings using the weights provided by the ICA decomposition (Mantini et al., 2007a). The artifact-corrected EEG signals were averaged with respect to rare and frequent event instants (100 ms pre-stimulus and 600 ms post-stimulus time), in order to obtain ERPs. The resulting ERPs were used to calculate, for each electrode, an ERP signal-to-noise ratio (SNR), defined as the ratio between the maximum amplitude in the post-stimulus interval and the root mean square (RMS) in the prestimulus interval.

P300 response time-course

After artifact attenuation, the EEG traces were used to measure the variations of the P300 response across trials. We used signals from a region of interest (ROI) over the scalp, including electrodes Cz, CP1, CP2, Pz, P3, P4, because they proved to consistently reflect this event-related activity (Picton, 1992). A P300 response time-course was calculated for each subject and each EEG signal, according to the procedure described hereafter. For the i-th trial, with $i = 1,…N$, the time instant t_i corresponding to a maximum in the EEG signal was detected in the 300–400 ms post-stimulus interval; then, a P300 wave template p was calculated averaging the single-trial responses k_i across the time window [t_i–150 ms; t_i+150 ms], selecting only those corresponding to rare stimuli. Then, the template p was compared with each trial response k_i, including both rare and frequent events, in the time window [t_i–150 ms; t_i+150 ms], and the P300 response intensity a_i was estimated by means of a least-squares fit of $a_i p$ with respect to k_i. After calculating the P300 response time-courses for each of the 6 selected electrodes, a global P300 response time-course was calculated by averaging them. In order to obtain a P300 reference time-course for EEG–fMRI correlation analysis, the global P300 response time-course was convolved with a canonical hemodynamic response function (HRF), generated using a gamma function (delay time, 2 s; rise time, 4 s; fall time, 6 s; undershoot, 0.2; restore time, 2 s). Finally, the P300 reference time-course was normalized by subtracting the minimum value and dividing by the difference of maximum and minimum values.

Separation of BOLD spatio-temporal patterns

Brain Voyager QX 1.9 (Brain Innovation, Maastricht, The Nederlands) was used for image data preparation and processing. The first 3 functional volumes were discarded to ensure steady-state longitudinal magnetization. The remaining functional image time-series were first corrected for the differences in slice acquisition times, detrended, realigned with T1-volumes and transformed into the standard Talairach anatomical space (Talairach and Tournoux, 1988). For each dataset, spatial ICA was applied to the fMRI time-series (McKeown at al., 1998). After data reduction by means of principal component analysis (PCA), ICs were estimated by means of the FastICA algorithm (Hyvärinen, 1999). Each fMRI IC consisted of a waveform and a spatial map: the waveform corresponded to the

time-course of the specific pattern; the intensity of this activity across voxels was expressed by the associated spatial map. To display voxels contributing most strongly to a particular IC and to allow inter-subject comparison, the intensity values in each map were scaled to z-scores (McKeown et al., 1998). In general, the spatial maps were characterized by areas with positive and negative z-scores, assumed to reflect stimulation-induced activation and deactivation, respectively.

In order to extend the ICA analysis from single-subject to multisubject study, the ICs estimated from each subject were clustered, matching the most similar spatial patterns across subjects. The self-organizing group ICA (sogICA) method, implemented in Brain Voyager QX, was used (Esposito et al., 2005). Once the ICs belonging to a cluster had been retrieved, the average spatial map was computed and assumed as representative for the cluster. The consistency of the clusters was expressed in terms by an intra-cluster similarity index s, defined as the average of the pair-wise spatial correlations between the constituting IC maps. The condition $s>0.10$ was used to select the clusters with reproducible maps across subjects. The remaining clusters were checked, analyzing also their single-subject maps. The exclusion of clusters that could be associated with artifacts was performed on the basis of the IC-fingerprint method (De Martino et al., 2007), as implemented in BrainVoyager QX.

With the intention of appreciating the different activations revealed by the EEG–fMRI analysis in terms of spatial maps, we also analyzed BOLD data with a classical approach (Linden et al., 1999), based on a rare/frequent contrast, and also with a more recent approach based on direct P300-BOLD correlation (Eichele et al., 2005; Horovitz et al., 2002). A general linear model (GLM) analysis (Friston et al., 1995) was performed for both of them, using different predictors. In the first case, the predictor was created convolving a time-course containing 0 for frequent events and 1 for rare events with the same HRF defined previously. In the second case, the P300 reference time-course was used as predictor. Fixed-effect analysis was used for obtaining group-level maps for both the rare/frequent contrast and P300-BOLD correlation methods. This allowed comparing the resulting maps, by means of the spatial correlation coefficient, with the ICA group maps, which were intrinsically based on a fixed-effect analysis.

Identification of brain networks linked to P300

The correspondence between the fluctuation of the P300 response and the activity of the fMRI networks was analyzed, estimating the similarity between the P300 reference time-course and the network time-courses. Specifically, the correlation coefficient r_p was computed for each subject. Since the correlation coefficients of the ICs that composed a specific cluster were not normally distributed, they were converted to z values using Fisher's r-to-z transformation (Zar, 1996). They were averaged, and the resulting value was back-transformed to r-values. A minimum correlation coefficient level to ensure statistical significance was determined using the two-tailed Pearson test ($p<0.05$ corrected). Accordingly, only the fMRI networks with $r_p>0.20$, were considered to be significantly related to the P300 response. In addition, we performed for each network a random-effect analysis on the z-scores by means of t-statistics, to measure the consistency of the correlations across subjects (Zar, 1996).

Results

The subjects recruited for the present study underwent a simple target detection experiment, consisting of a visual oddball paradigm (Supplementary Fig. 1), with mental counting of the occurrence of rare events. After the simultaneous EEG–fMRI acquisition, they all correctly reported the number of visual targets.

After the attenuation of BCG, imaging and ocular artifacts (Fig. 1), single-subject EEG data collected during simultaneous fMRI scanning were analyzed. ERP scalp topography and scalp maps at P300 latency showed a major contribution of the P300 component over the centro-parietal region, with latency in the 300–400ms range (Fig. 2). Early N1 and P1 components could also be observed in the ERP, although they were weaker than the P300 component. The analysis of the ERP SNR across subjects, in line with the spatial distribution of the P300 component, showed a bilateral pattern, more prominent at P3 and P4 electrodes (Supplementary Fig. 2). Electrophysiological measures of the ongoing cerebral activity related to target detection were obtained by single-trial analysis of the P300 responses (Fig. 3 and Supplementary Fig. 3). Raster plots of time-locked responses at electrode Pz were generated for all trials together, and for rare and frequent events separately (Figs. 3a and b, respectively). The latter clearly revealed differences among the two groups in terms of event-related electric activity at the latency of about 350 ms, which corresponded to the P300 component. The P300 response across trials, obtained comparing the single epochs with the ERP (Supplementary Fig. 3), showed significantly larger intensity for rare than for frequent events (Fig. 3c). A P300 reference time-course for EEG–fMRI correlation analysis could be obtained from the P300 response variations by convolution with a canonical HRF (Fig. 3d). The P300 response time-course calculated using a selection of electrodes over the centro-parietal region showed a large correspondence with those separately extracted from the constituting electrodes (Supplementary Fig. 4), with an average correlation across subjects ranging between 0.90 and 0.94.

With regard to fMRI data analysis, we identified five fMRI IC clusters, which were associated with the dorsal attention, the ventral attention, the core, the visual and the sensory-motor networks (Fig. 4 and Supplementary Fig. 5). Their spatial patterns were consistent across subjects, with intra-cluster similarity ranging between 0.15 and 0.28. Other fMRI clusters were produced by our analysis, but were not further analyzed because they were associated with artifacts, or were almost inconsistent across subjects (Supplementary Fig. 6). The ventral attention network mainly included the right temporo-parietal junction, inferior and middle frontal gyrus, and anterior cingulate; the areas of this network showed to be anti-correlated with posterior–lateral and midline regions that are commonly more active at rest, and correspond to the default-mode network (Supplementary Table 1). The dorsal attention network mainly included the intraparietal sulcus, the frontal eye field (FEF), and the middle frontal gyrus (Supplementary Table 2). The core network mainly included the anterior cingulate, the bilateral insular and dorso-lateral prefrontal cortices. The visual network included the retinotopic occipital cortex and temporal–occipital regions dedicated to visual processing. The sensory-motor network included the precentral, postcentral, and medial frontal gyri, the primary sensory-motor cortices, and the supplementary motor area. Among these five brain networks, only the ventral and the dorsal attention networks were

found to be significantly correlated with the P300 reference time-course (Table 1). Analysis of the time-averaged network response (fMRI activation) to the presentation of targets showed that only the ventral attention network consistently responded to the rare stimuli, whereas the averaging procedure seemed to attenuate the signals of the dorsal attention network (Fig. 4). In addition, event-related responses were observed for the visual network and the core network, with larger intensity and shorter duration for the former one, whereas the activity of the sensory-motor network did not seem to be time-locked to the stimulus presentation.

Analyzing the fMRI data with the classical approach based on a rare/frequent contrast, as well as with the P300-BOLD correlation approach, we obtained spatial maps that seemed to be quite consistent with the ICA results (Supplementary Fig. 7). The rare/frequent contrast map included brain activations in the thalamus, the midbrain, the middle/superior frontal gyrus, the supplementary motor area, the precentral gyrus, the middle temporal gyrus, the inferior and superior parietal lobules, the precuneus and the cuneus (Supplementary Table 3). Conversely, the P300-BOLD correlation map mainly showed the involvement of the insula, the middle frontal gyrus, the anterior cingulate, the supplementary motor area, the precentral gyrus, the middle temporal gyrus, and the inferior parietal lobule, the precuneus and the cuneus (Supplementary Table 4). Comparing the ICA network maps with that of the rare/frequent contrast analysis, we observed a large correspondence areas for activations in the ventral attention network, with a spatial correlation of 0.51 (p<0.001), and a minor overlap for those in the dorsal attention network, with a spatial correlation of 0.10 (p<0.001). By contrast, the P300-fMRI correlation map showed stronger correspondence with the dorsal than with the ventral attention network, with a correlation of 0.34 (p<0.001) and 0.21 (p<0.001) respectively. Activations obtained with the classical and the correlation-based approaches within visual and motor areas were found to be present in the two corresponding networks separated by ICA, but our EEG–fMRI analysis revealed them as not significantly correlated with the P300 response fluctuations (Table 1).

Discussion

Brain activity during target detection was decomposed into coherent spatio-temporal patterns, that were investigated using a data-driven approach, linking P300 response variations and BOLD coherent fluctuations.

Methodological considerations

Since the EEG recordings collected in the MRI scanner were contaminated by imaging, BCG, and ocular artifacts, we applied artifact attenuation techniques to obtain signals that could be useful for EEG–fMRI integration. Given that EEG and fMRI were recorded simultaneously, we used the slice-based AAS method for artifact imaging subtraction (Gonçalves et al., 2007), thus avoiding a possible P300 attenuation induced by the classical gradient-based AAS method (Allen et al., 2000). The residual imaging contamination in our EEG data, as well as the BCG and ocular artifacts, were then removed by means of an ICA-based procedure, which was already tested and used in our previous EEG–fMRI studies (Mantini et al., 2007a,b).

In previous studies, after artifact attenuation the EEG data were typically used for ERP analysis, based on electromagnetic source localizations at different latencies (Goldstein et al., 2002). Accordingly, the single epochs were averaged, and therefore their variability was not taken into account. In our study, this analysis revealed an important contribution of the P300 component to the ERP, in particular at the centro-parietal electrodes, whereas we generally observed weak P1 and N1 responses, probably due to our specific experimental paradigm. Since we observed a SNR sufficient for single-trial analysis of the P300 component, we measured its trial-by-trial response fluctuations. This information, considered to indirectly allow off-line monitoring of target detection performance (Debener et al., 2005), was particularly valuable. Other authors reported that the P300 amplitude variability was affected by inter-stimulus interval (Sambeth et al., 2004), target-to-target interval (Gonsalvez and Polich, 2002), or target probability (Croft et al., 2003). However, no clear indication about the cerebral mechanisms accounting for the P300 response fluctuations observed during the oddball task could be provided in these studies. We analyzed the trial-by-trial responses recorded by EEG–fMRI to obtain an indirect measure of both the electrophysiological and the hemodynamic correlates of brain activity linked to target detection. In our study, the P300 reference time-course from EEG single trials (Horovitz et al., 2002) was primarily used to interpret the results from the fMRI data.

In order to identify and characterize cortical responses to the stimuli, traditional fMRI data-analysis methods require knowledge of stimulus timing, or of a region of interest (Friston et al. 1995). In the perspective of EEG–fMRI integration, we aimed at developing a method for the fusion of information from electrophysiological and hemodynamic measures of ongoing cerebral processes. To this purpose, we analyzed fMRI images by means of ICA, a signal processing method able to separate independent spatio-temporal patterns of brain activity (Hyvärinen and Oja, 2000; James and Hesse, 2005). ICA allowed the decomposition of observations into independent patterns, without any prior knowledge about their activity waveforms or locations (McKeown et al., 1998). Due to its characteristics, ICA demonstrated to be a powerful tool for the extraction of functional connectivity patterns of synchronized neural activity, and in particular for the retrieval of functionally distinct cerebral networks (Bartels and Zeki, 2005; Beckmann et al., 2005).

Since the ICA method permitted the separation of a number of functionally distinct coherence patterns for each dataset, we used the sogICA method, in order to produce group inferences in a multi-subject analysis (Esposito et al., 2005). By means of this second-level analysis, we could also find reproducible spatial patterns across subjects. Moreover, information in the time-domain was not discarded during the clustering process; rather, the time-courses of brain activation for the ICs belonging to the same cluster were grouped and jointly analyzed for measuring the correlation of the specific network with the P300 reference time-course.

Our EEG–fMRI method based on ICA for fMRI analysis allowed linking information from EEG and fMRI data according to a data-driven approach. Therefore, it can be assumed to be unbiased by the use of an incomplete model for the fusion of EEG and fMRI data. For example, although we extracted only the most prominent feature from the EEG data (the P300 component), we could relate the P300 response variations with the network ongoing

activity. Conversely, the use of the P300 reference time-course in a hypothesis-driven EEG-based GLM analysis would not generally provide complete information, because it would strictly require, instead, a set of EEG predictors capable to comprehensively account for the fMRI time-courses. The present study showed that the EEG-informed fMRI analysis can be effectively conducted by ICA of fMRI data, just as previous studies by Debener showed that it can benefit from ICA of EEG data (Debener et al., 2005, 2006). The next logical step would be to use ICA on both EEG and fMRI. From this standpoint, Eichele suggested to use ICA in parallel on simultaneously acquired EEG and fMRI data, and to match the ICA results by correlating the EEG and fMRI IC trial-to-trial modulations (Eichele et al., 2008). Subsequently, Moosmann proved in a simulation study that the decomposition of simultaneously recorded single-trial EEG–fMRI data in the same ICA model might be feasible (Moosmann et al., 2008). It is our opinion that a possible methodological development in the perspective of simultaneous EEG–fMRI integration may be the use of self-organized clustering with both the EEG ICs and the fMRI ICs, and then the association of the EEG and fMRI clusters using spatial and temporal information.

Neurobiological considerations

It was recently observed that the local field potential (LFP) correlates with the BOLD signal (Leopold et al., 2003; Logothetis et al., 2001). Since the LFP is the basis for scalp EEG, a non-invasive method for multimodal integration could be achieved by investigating correlations between BOLD and EEG responses (Horovitz et al., 2002; Benar et al., 2007). Our approach provided additional information with respect to previous EEG–fMRI studies based on fMRI-constrained source localization of ERPs (Moores et al., 2003; Mulert et al., 2004), or on direct ERP/fMRI integration (Calhoun et al., 2006), and complemented the results of classical fMRI statistical analyses (Linden et al., 1999). These showed a large number of P300 generators, specifically in the supplementary motor area, the anterior cingulate, the middle and superior frontal cortex, the insula, the posterior parietal cortex, and the right temporo-parietal junction, which were suggested to belong to different functional systems (Bledowski et al., 2004a; Horn et al., 2003).

Using information from concurrent EEG and fMRI, our method permitted separating and charactering the activity of the ventral attention, the dorsal attention, the core, the visual and the sensory-motor networks, as previously defined in neuroimaging studies on active and passive behavioral tasks (Corbetta and Shulman, 2002; Dosenbach et al., 2006; Fox et al., 2006; Nir et al., 2006). Among them, the first two proved to be consistently related to target detection processes. The ventral attention network included brain areas that were activated by the presentation of the rare stimuli, and other areas that were concurrently deactivated. Activation in the ventral attention system was associated with the detection of behaviorally relevant and unexpected stimuli, and, more generally, of changes in the sensory environment (Corbetta and Shulman, 2002; Downar et al., 2000). It was reported to be independent of the presentation modality, and to be significantly right-lateralized (Downar et al., 2000). The same set of brain areas was also specifically and consistently found to be associated with transient responses at task onset and offset (Fox et al., 2005; Konishi et al., 2001), an effect thought to be related to transitions from and to a state of readiness (Corbetta and Shulman, 2002; Shulman et al., 2002). Deactivations were mainly found in precuneus, medial

prefrontal cortex and medial parietal cortex,. All these areas, typically associated with the default-mode system, were shown to be more active during rest, and to be transiently or consistently deactivated during many different types of cognitive tasks (Shulman et al., 1997; Binder et al., 1999). The dorsal attention network, characterized by the involvement of parietal and prefrontal regions, was usually engaged during voluntary orienting (Corbetta and Shulman, 2002). Interestingly, our analysis revealed that the time-course of this network reflected a modulation that was averaged out if time-locked to the presentation of targets, but was nevertheless correlated with the P300 response fluctuations across trials. This specific system was previously found to be related to P300 responses by Eichele and colleagues, who combined the ERP response at different latencies with the simultaneously acquired BOLD signals by means of a modified auditory oddball paradigm (Eichele et al., 2005). This result was also confirmed by our findings: the high spatial correlation between the maps of the dorsal attention network and the P300-BOLD correlation analysis is an indication that the P300 response fluctuations were modulated by brain intrinsic activity (Fox et al., 2006; 2007). This activity was suggested to be driven, to some extent, by behavioral conditions (Fox et al., 2007; Fox and Raichle, 2007). In particular the dorsal attention network was supposed to be influenced by voluntary attention shifts during search for salient stimuli (Shulman et al., 2003). Furthermore, other neuroimaging studies demonstrated that the activation of this specific network largely reflected sustained activity during continuous cognitive and behavioral tasks (Fox et al., 2005; Visscher et al., 2003), presumably related to adaptive task control (Dosenbach et al., 2007).

In conclusion, in this study we linked the cerebral dynamics observed through EEG and fMRI, for investigating the different contribution of distinct cortical networks to target detection. It is our opinion that the analysis of single trials, as supported by this study, may provide information beyond what can be revealed by the analysis of trial averages. This information can be potentially valuable, mostly when applied to the trial-by-trial coupling of concurrent electrophysiological and hemodynamic cerebral measures, for further investigations on cognitive functions related to sensory processing, attention and memory.

Supplementary Material

Refer to Web version on PubMed Central for supplementary material.

Acknowledgments

References

Allen PJ, Josephs O, Turner R. A method for removing imaging artifact from continuous EEG recorded during functional MRI. NeuroImage. 2000; 12:230–239. [PubMed: 10913328]

Arieli A, Sterkin A, Grinvald A, Aertsen A. Dynamics of ongoing activity: explanation of the large variability in evoked cortical responses. Science. 1996; 273:1868–1871. [PubMed: 8791593]

Barry RJ, Kirkaikul S, Hodder D. EEG alpha activity and the ERP to target stimuli in an auditory oddball paradigm. Int. J. Psychophysiol. 2000; 39:39–50. [PubMed: 11120346]

Bartels A, Zeki S. The chronoarchitecture of the cerebral cortex. Philos. Trans. R. Soc. Lond. B. Biol. Sci. 2005; 360:733–750. [PubMed: 15937010]

Basile LF, Rogers RL, Simos PG, Papanicolaou AC. Magnetoencephalographic evidence for common sources of long latency fields to rare target and rare novel visual stimuli. Int. J. Psychophysiol. 1997; 25:123–137. [PubMed: 9101337]

Beckmann CF, De Luca M, Devlin JT, Smith SM. Investigations into resting-state connectivity using independent component analysis. Philos. Trans. R. Soc. Lond. B. Biol. Sci. 2005; 360:1001–1013. [PubMed: 16087444]

Benar CG, Schon D, Grimault S, Nazarian B, Burle B, Roth M, Badier JM, Marquis P, Liegeois-Chauvel C, Anton JL. Single-trial analysis of oddball event-related potentials in simultaneous EEG–fMRI. Hum. Brain. Mapp. 2007; 28:602–613. [PubMed: 17295312]

Binder JR, Frost JA, Hammeke TA, Bellgowan PS, Rao SM, Cox RW. Conceptual processing during the conscious resting state. A functional MRI study. J. Cogn. Neurosci. 1999; 11:80–95. [PubMed: 9950716]

Blackwood D. P300, a state and a trait marker in schizophrenia. Lancet. 2000; 355:771–772. [PubMed: 10711922]

Bledowski C, Prvulovic D, Goebel R, Zanella FE, Linden DE. Attentional systems in target and distractor processing: a combined ERP and fMRI study. Neuroimage. 2004a; 22:530–540. [PubMed: 15193581]

Bledowski C, Prvulovic D, Hoechstetter K, Scherg M, Wibral M, Goebel R, Linden DE. Localizing P300 generators in visual target and distractor processing: a combined event-related potential and functional magnetic resonance imaging study. J. Neurosci. 2004b; 24:9353–9360. [PubMed: 15496671]

Calhoun VD, Adali T, Pearlson GD, Kiehl KA. Neuronal chronometry of target detection: fusion of hemodynamic and event-related potential data. Neuroimage. 2006; 30:544–553. [PubMed: 16246587]

Clark VP, Fannon S, Lai S, Benson R, Bauer L. Responses to rare visual target and distractor stimuli using event-related fMRI. J. Neurophysiol. 2000; 83:3133–3139. [PubMed: 10805707]

Croft RJ, Gonsalvez CJ, Gabriel C, Barry RJ. Target-to-target interval versus probability effects on P300 in one- and two-tone tasks. Psychophysiology. 2003; 40:322–328. [PubMed: 12946107]

Corbetta M, Shulman GL. Control of goal-directed and stimulus-driven attention in the brain. Nat. Rev. Neurosci. 2002; 3:201–215. [PubMed: 11994752]

Damoiseaux JS, Rombouts SA, Barkhof F, Scheltens P, Stam CJ, Smith SM, Beckmann CF. Consistent resting-state networks across healthy subjects. Proc. Natl. Acad. Sci. U. S. A. 2006; 103:13848–13853. [PubMed: 16945915]

Debener S, Ullsperger M, Siegel M, Fiehler K, von Cramon DY, Engel AK. Trial-by-trial coupling of concurrent electroencephalogram and functional magnetic resonance imaging identifies the dynamics of performance monitoring. J. Neurosci. 2005; 25:11730–11737. [PubMed: 16354931]

Debener S, Ullsperger M, Siegel M, Engel AK. Single-trial EEG–fMRI reveals the dynamics of cognitive function. Trends Cogn. Sci. 2006; 10:558–563. [PubMed: 17074530]

De Luca M, Beckmann CF, De Stefano N, Matthews PM, Smith SM. fMRI resting state networks define distinct modes of long-distance interactions in the human brain. Neuroimage. 2006; 29:1359–1367. [PubMed: 16260155]

De Martino F, Gentile F, Esposito F, Balsi M, Di Salle F, Goebel R, Formisano E. Classification of fMRI independent components using IC-fingerprints and support vector machine classifiers. Neuroimage. 2007; 34:177–194. [PubMed: 17070708]

Dosenbach NU, Visscher KM, Palmer ED, Miezin FM, Wenger KK, Kang HC, Burgund ED, Grimes AL, Schlaggar BL, Petersen SE. A core system for the implementation of task sets. Neuron. 2006; 50:799–812. [PubMed: 16731517]

Dosenbach NU, Fair DA, Miezin FM, Cohen AL, Wenger KK, Dosenbach RA, Fox MD, Snyder AZ, Vincent JL, Raichle ME, Schlaggar BL, Petersen SE. Distinct brain networks for adaptive and stable task control in humans. Proc. Natl. Acad. Sci. U. S. A. 2007; 104:11073–11078. [PubMed: 17576922]

Downar J, Crawley AP, Mikulis DJ, Davis KD. A multimodal cortical network for the detection of changes in the sensory environment. Nat. Neurosci. 2000; 3:277–283. [PubMed: 10700261]

Eichele T, Specht K, Moosmann M, Jongsma ML, Quiroga RQ, Nordby H, Hugdahl K. Assessing the spatiotemporal evolution of neuronal activation with single-trial event-related potentials and functional MRI. Proc. Natl. Acad. Sci. U. S. A. 2005; 102:17798–17803. [PubMed: 16314575]

Eichele T, Calhoun VD, Moosmann M, Specht K, Jongsma ML, Quiroga RQ, Nordby H, Hugdahl K. Unmixing concurrent EEG–fMRI with parallel independent component analysis. Int. J. Psychophysiol. 2008; 67:222–234. [PubMed: 17688963]

Esposito F, Scarabino T, Hyvärinen A, Himberg J, Formisano E, Comani S, Tedeschi G, Goebel R, Seifritz E, Di Salle F. Independent component analysis of fMRI group studies by self-organizing clustering. Neuroimage. 2005; 25:193–205. [PubMed: 15734355]

Fair DA, Schlaggar BL, Cohen AL, Miezin FM, Dosenbach NU, Wenger KK, Fox MD, Snyder AZ, Raichle ME, Petersen SE. A method for using blocked and event-related fMRI data to study "resting state" functional connectivity. Neuroimage. 2007; 35:396–405. [PubMed: 17239622]

Fox MD, Raichle ME. Spontaneous fluctuations in brain activity observed with functional magnetic resonance imaging. Nat. Rev. Neurosci. 2007; 8:700–711. [PubMed: 17704812]

Fox MD, Snyder AZ, Barch DM, Gusnard DA, Raichle ME. Transient BOLD responses at block transitions. Neuroimage. 2005; 28:956–966. [PubMed: 16043368]

Fox MD, Snyder AZ, Zacks JM, Raichle ME. Coherent spontaneous activity accounts for trial-to-trial variability in human evoked brain responses. Nat. Neurosci. 2006; 9:23–25. [PubMed: 16341210]

Fox MD, Snyder AZ, Vincent JL, Raichle ME. Intrinsic fluctuations within cortical systems account for intertrial variability in human behavior. Neuron. 2007; 56:171–184. [PubMed: 17920023]

Friston KJ, Holmes AP, Worsley KP, Poline JB, Frith CD, Frackowiak RS. Statistical parametric maps in functional imaging: a general linear approach. Hum. Brain. Mapp. 1995; 2:189–210.

Goldstein A, Spencer KM, Donchin E. The influence of stimulus deviance and novelty on the P300 and novelty P3. Psychophysiology. 2002; 39:781–790. [PubMed: 12462506]

Gonsalvez CL, Polich J. P300 amplitude is determined by target-to-target interval. Psychophysiology. 2002; 39:388–396. [PubMed: 12212658]

Gonçalves SI, Pouwels PJ, Kuijer JP, Heethaar RM, de Munck JC. Artifact removal in co-registered EEG–fMRI by selective average subtraction. Clin. Neurophysiol. 2007; 118:2437–2450. [PubMed: 17889599]

Halgren E, Marinkovic K, Chauvel P. Generators of the late cognitive potentials in auditory and visual oddball tasks. Electroencephalogr. Clin. Neurophysiol. 1998; 106:156–164. [PubMed: 9741777]

Hyvärinen A. Fast and robust fixed-point algorithms for independent component analysis. IEEE Trans. Neural Networks. 1999; 10:626–634. [PubMed: 18252563]

Hyvärinen A, Oja E. Independent component analysis: algorithms and applications. Neural Netw. 2000; 13:411–430. [PubMed: 10946390]

Horn H, Syed N, Lanfermann H, Maurer K, Dierks T. Cerebral networks linked to the event-related potential P300. Eur. Arch. Psychiatry Clin. Neurosci. 2003; 253:154–159. [PubMed: 12904980]

Horovitz SG, Skudlarski P, Gore JC. Correlations and dissociations between BOLD signal and P300 amplitude in an auditory oddball task: a parametric approach to combining fMRI and ERP. Magn. Reson. Imaging. 2002; 20:319–325. [PubMed: 12165350]

James CJ, Hesse CW. Independent component analysis for biomedical signals. Physiol. Meas. 2005; 26:R15–R39. [PubMed: 15742873]

Katsarou Z, Bostantjopoulou S, Kimiskidis V, Rossopoulos E, Kazis A. Auditory event-related potentials in Parkinson's disease in relation to cognitive ability. Percept. Mot. Skills. 2004; 98:1441–1448. [PubMed: 15291236]

Kiehl KA, Stevens MC, Laurens KR, Pearlson G, Calhoun VD, Liddle PF. An adaptive reflexive processing model of neurocognitive function: supporting evidence from a large scale ($n = 100$) fMRI study of an auditory oddball task. Neuroimage. 2005; 25:899–915. [PubMed: 15808990]

Konishi S, Donaldson DI, Buckner RL. Transient activation during block transition. Neuroimage. 2001; 13:364–374. [PubMed: 11162276]

Leopold DA, Murayama Y, Logothetis NK. Very slow activity fluctuations in monkey visual cortex: implications for functional brain imaging. Cereb. Cortex. 2003; 13:422–433. [PubMed: 12631571]

Lew GS, Polich J. P300, habituation, and response mode. Physiol. Behav. 1993; 53:111–117. [PubMed: 8434050]

Linden DE, Prvulovic D, Formisano E, Vollinger M, Zanella FE, Goebel R, Dierks T. The functional neuroanatomy of target detection: an fMRI study of visual and auditory oddball tasks. Cereb. Cortex. 1999; 9:815–823. [PubMed: 10601000]

Logothetis NK, Pauls J, Augath M, Trinath T, Oeltermann A. Neurophysiological investigation of the basis of the fMRI signal. Nature. 2001; 412:150–157. [PubMed: 11449264]

Makeig S, Jung TP, Bell AJ, Ghahremani D, Sejnowski TJ. Blind separation of auditory event-related brain responses into independent components. Proc. Natl. Acad. Sci. U. S. A. 1997; 94:10979–10984. [PubMed: 9380745]

Makeig S, Westerfield M, Jung TP, Enghoff S, Townsend J, Courchesne E, Sejnowski TJ. Dynamic brain sources of visual evoked responses. Science. 2002; 295:690–694. [PubMed: 11809976]

Makeig S, Debener S, Onton J, Delorme A. Mining event-related brain dynamics. Trends Cogn. Sci. 2004; 8:204–210. [PubMed: 15120678]

Mantini D, Perrucci MG, Cugini S, Ferretti A, Romani GL, Del Gratta C. Complete artifact removal for EEG recorded during continuous fMRI using independent component analysis. Neuroimage. 2007a; 34:598–607. [PubMed: 17112747]

Mantini D, Perrucci MG, Del Gratta C, Romani GL, Corbetta M. Electrophysiological signatures of resting state networks in the human brain. Proc. Natl. Acad. Sci. U. S. A. 2007b; 104:13170–13175. [PubMed: 17670949]

McKeown MJ, Makeig S, Brown GG, Jung TP, Kindermann SS, Bell AJ, Sejnowski TJ. Analysis of fMRI data by blind separation into independent spatial components. Hum. Brain. Mapp. 1998; 6:160–188. [PubMed: 9673671]

Moores KA, Clark CR, Hadfield JL, Brown GC, Taylor DJ, Fitzgibbon SP, Lewis AC, Weber DL, Greenblatt R. Investigating the generators of the scalp recorded visuo-verbal P300 using cortically constrained source localization. Hum. Brain. Mapp. 2003; 18:53–77. [PubMed: 12454912]

Moosmann M, Eichele T, Nordby H, Hugdahl K, Calhoun VD. Joint independent component analysis for simultaneous EEG–fMRI: principle and simulation. Int. J. Psychophysiol. 2008; 67:212–221. [PubMed: 17688965]

Mulert C, Jager L, Schmitt R, Bussfeld P, Pogarell O, Moller HJ, Juckel G, Hegerl U. Integration of fMRI and simultaneous EEG: towards a comprehensive understanding of localization and time-course of brain activity in target detection. Neuroimage. 2004; 22:83–94. [PubMed: 15109999]

Muscoso EG, Costanzo E, Daniele O, Maugeri D, Natale E, Caravaglios G. Auditory event-related potentials in subcortical vascular cognitive impairment and in Alzheimer's disease. J. Neural Transm. 2006; 113:1779–1786. [PubMed: 17039300]

Nir Y, Hasson U, Levy I, Yeshurun Y, Malach R. Widespread functional connectivity and fMRI fluctuations in human visual cortex in the absence of visual stimulation. Neuroimage. 2006; 30:1313–1324. [PubMed: 16413791]

Picton TW. The P300 wave of the human event-related potential. J. Clin. Neurophysiol. 1992; 9:456–479. [PubMed: 1464675]

Polich J, Herbst KL. P300 as a clinical assay: rationale, evaluation, and findings. Int. J. Psychophysiol. 2000; 38:3–19. [PubMed: 11027791]

Polich J, Kok A. Cognitive and biological determinants of P300: an integrative review. Biol. Psychol. 1995; 41:103–146. [PubMed: 8534788]

Sambeth A, Maes JH, Brankack J. With long intervals, inter-stimulus interval is the critical determinant of the human P300 amplitude. Neurosci. Lett. 2004; 359:143–146. [PubMed: 15050684]

Shulman GL, Fiez JA, Corbetta M, Buckner RL, Miezin FM, Raichle ME, Petersen SE. Common blood flow changes across visual tasks: II. Decreases in cerebral cortex. J. Cogn. Neurosci. 1997; 9:648–663. [PubMed: 23965122]

Shulman GL, d'Avossa G, Tansy AP, Corbetta M. Two attentional processes in the parietal lobe. Cereb. Cortex. 2002; 12:1124–1131. [PubMed: 12379601]

Shulman GL, McAvoy MP, Cowan MC, Astafiev SV, Tansy AP, d'Avossa G, Corbetta M. Quantitative analysis of attention and detection signals during visual search. J. Neurophysiol. 2003; 90:3384–3397. [PubMed: 12917383]

Strobel A, Debener S, Sorger B, Peters JC, Kranczioch C, Hoechstetter K, Engel AK, Brocke B, Goebel R. Novelty and target processing during an auditory novelty oddball: a simultaneous event-related potential and functional magnetic resonance imaging study. Neuroimage. 2008; 40:869–883. [PubMed: 18206391]

Talairach, J., Tournoux, P. Co-Planar Stereotaxic Atlas of the Human Brain. Thieme Medical Publishers; New York: 1988.

Tarkka IM, Stokic DS. Source localization of P300 from oddball, single stimulus, and omitted-stimulus paradigms. Brain. Topogr. 1998; 11:141–151. [PubMed: 9880172]

Visscher KM, Miezin FM, Kelly JE, Buckner RL, Donaldson DI, McAvoy MP, Bhalodia VM, Petersen SE. Mixed blocked/event-related designs separate transient and sustained activity in fMRI. Neuroimage. 2003; 19:1694–11708. [PubMed: 12948724]

Zar, JH. Biostatistical Analysis. Prentice-Hall; Upper Saddle River, NJ: 1996.
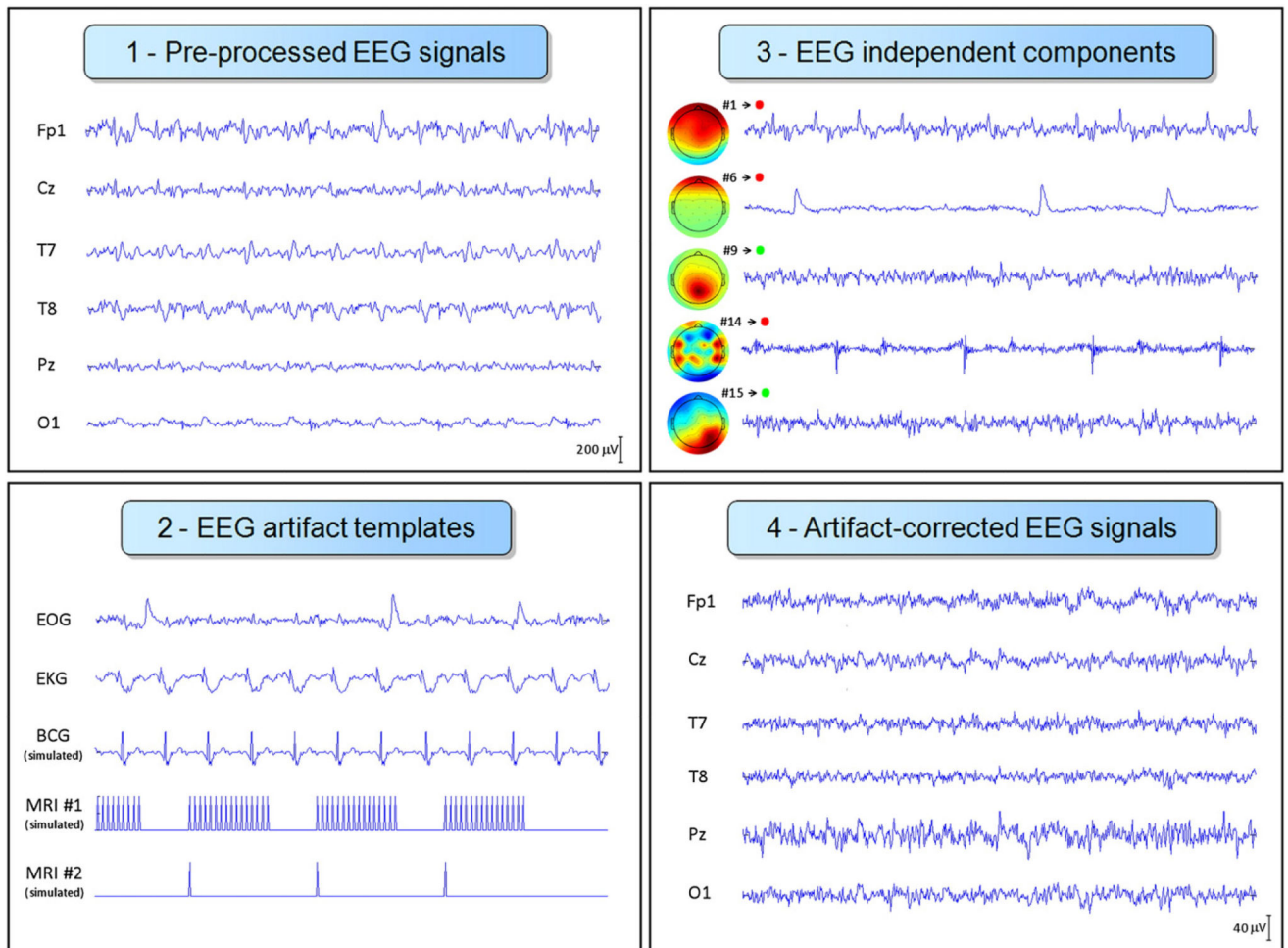
Fig.1.

ICA-based procedure for EEG artifact correction. (1) Pre-processed EEG signals are obtained by slice-based AAS method for imaging artifact attenuation, downsampling to 1 kHz and filtering in the band 0.5–40 Hz; (2) EEG artifact templates for subsequent artifact detection are prepared using the simultaneously recorded EOG and EKG, as well as simulated signals for BCG, slice MRI and volume MRI artifacts; (3) ICA full decomposition is performed on the pre-processed EEG data, and the resulting ICs are classified into brain signals and artifacts on the basis of the correlations with the EEG artifact templates; (4) Artifact-corrected EEG signals are obtained by subtracting the detected artifacts using the weights provided by the ICA decomposition.
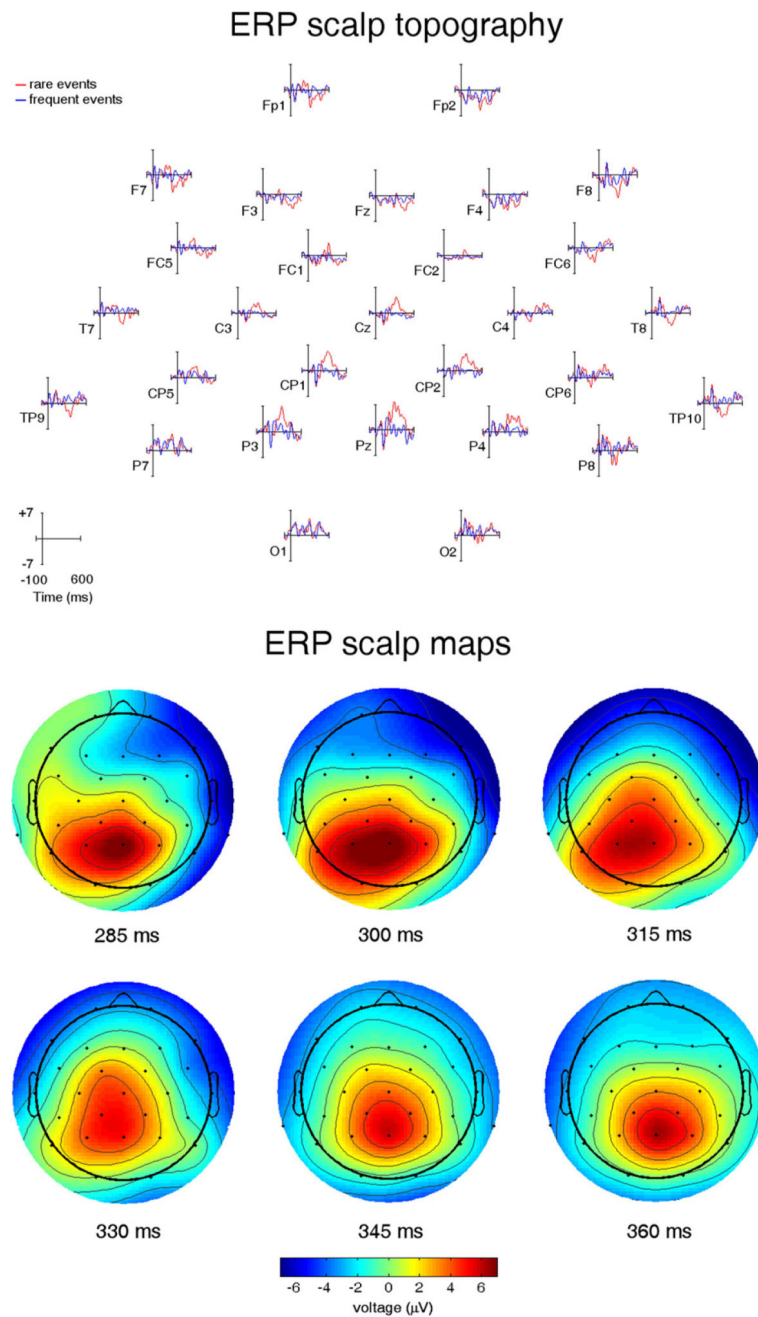
ERP scalp topography

ERP scalp maps

Fig. 2.
Single-subject ERP analysis of artifact-corrected EEG signals. (Top panel) Scalp topography of ERPs associated with rare and frequent events; (Bottom panel) Scalp maps showing the temporal evolution of the P300 response.
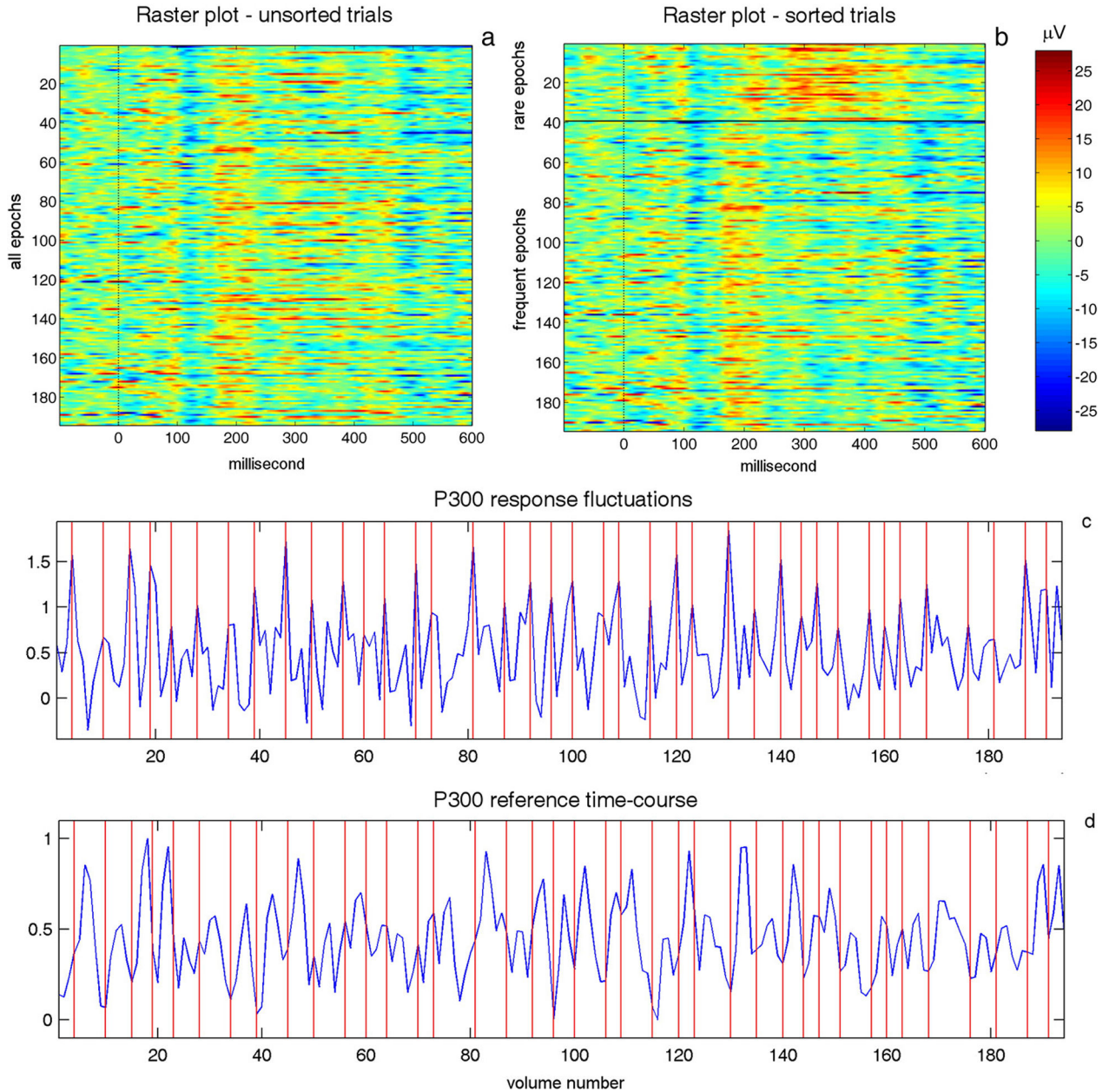
EEG single-trial analysis

Fig. 3.
Single-subject single-trial analysis of artifact-corrected EEG signals. (a) Raster plot of all trials at electrode Cz, aligned to stimulus onset, with electric potential expressed in color scale; (b) separate raster plots of trials at electrode Pz, corresponding to rare and frequent events; (c) reconstructed fluctuations of the P300 response across trials, with red bars placed in correspondence of rare events; (d) P300 reference time-course obtained from the convolution of the P300 response fluctuations with a canonical HRF.
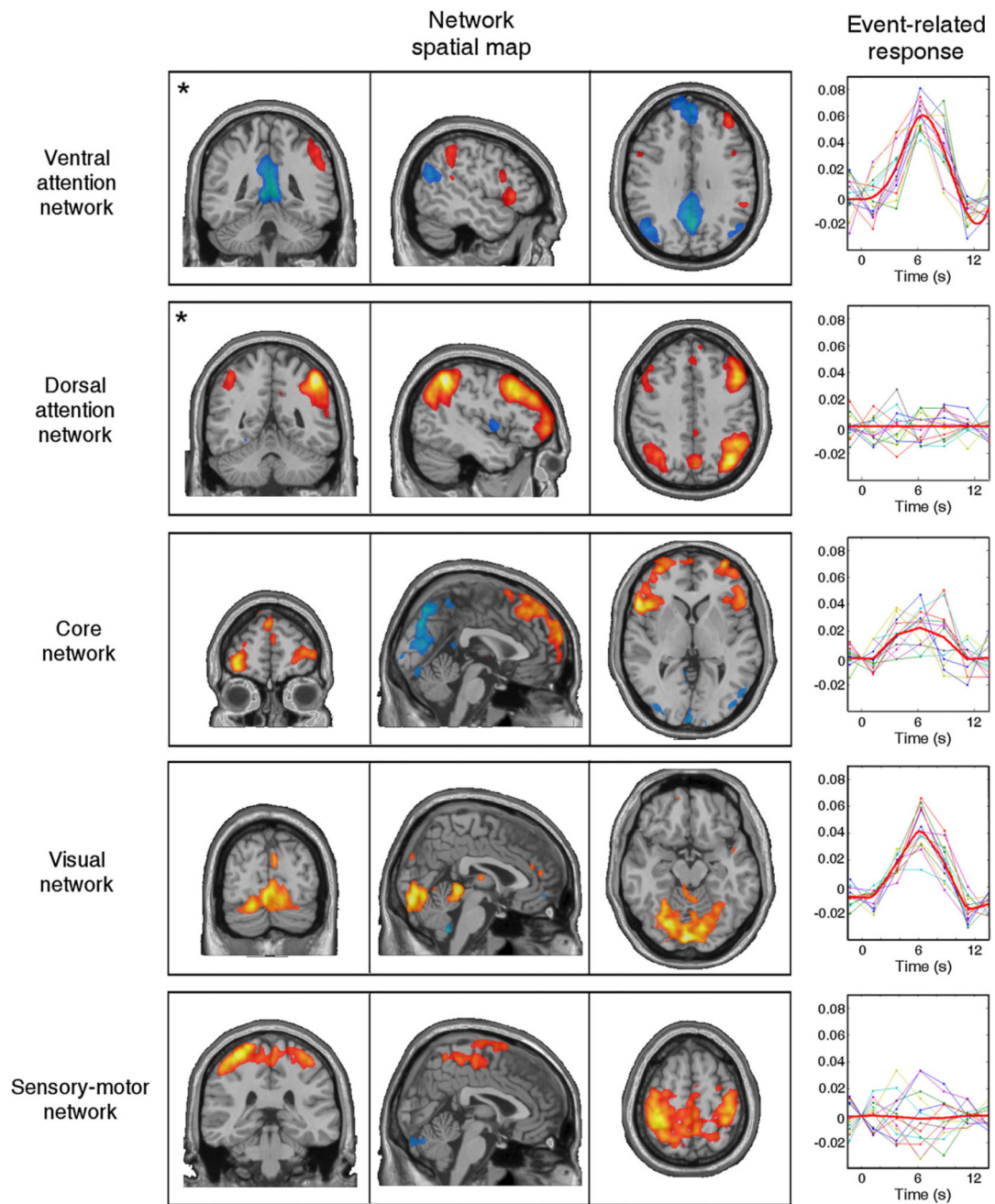
Fig. 4.
Spatio-temporal analysis of the five networks consistently found across subjects. The first two networks, marked with a star, are significantly correlated with the P300 response fluctuations. For each network, sagittal, coronal and axial maps are shown, along with the average time-courses in response to rare events. The maps contain regions with positive (warm colors, yellow-orange) or negative (cool colors, azure-blue) z-scores. The average time-courses are normalized because they refer to the average activity of the brain patterns. The thick red line in each graph represents the best-fit to all data points.

Table 1

Statistics on the correlations between the P300 reference time-course and the fMRI network time-courses

	Ventral attention network	Dorsal attention network	Core network	Visual network	Somatomotor network
Average correlation	0.27 *	0.23 *	0.04	−0.06	−0.04
Standard deviation	0.14	0.12	0.29	0.22	0.22
T-score	1.97 **	1.98 **	0.13	−0.25	−0.18

For each network, the average and the standard deviation across subjects is provided, along with the corresponding *t*-score value.

*
Significant correlation value (*p*<0.05, corrected for multiple comparison).

**
Significant *t*-score value (*p* < 0.05).